A Satellite Image Set for the Evolution of Image Transforms for Defense Applications

Michael R. Peterson
Dept. of Computer Science and Engineering
Wright State University
Dayton, OH, USA
peterson.7@wright.edu

Gary B. Lamont
Dept. of Electrical and Computer Engineering
U. S. Air Force Institute of Technology
WPAFB, OH, USA
gary.lamont@afit.edu

Frank Moore
Dept. of Mathematical Sciences
University of Alaska Anchorage
Anchorage, AK, USA
affwm@uaa.alaska.edu

Patrick Marshall
AFRL/IFTA
WPAFB, OH, USA
patrick.marshall@wpafb.af.mil

ABSTRACT

In recent years, wavelets have been widely applied in state-of-the-art image processing algorithms, providing efficient compression while maintaining superior image quality. However, wavelet performance may not be sufficient when extreme compression ratios are required. Defense applications often require robust transforms simultaneously minimizing bandwidth requirements and image resolution loss. Image processing algorithms take advantage of quantization to provide substantial lossy compression ratios at the expense of resolution. Recent research demonstrates that genetic algorithms (GAs) evolve filters outperforming standard discrete wavelet transforms in conditions subject to high quantization error. Evolved filters must be trained using images appropriate to their intended application. We present a set of fifty satellite images used to evolve image transforms appropriate for satellite and unmanned aerial vehicle (UAV) reconnaissance applications. We identify the best training and test images. Image transforms evolved using appropriate training images reduce the mean squared error (MSE) by an average of greater than 15% across the entire image set under conditions subject to high quantization error.

Categories and Subject Descriptors

I.2.8 [**Artificial Intelligence**]: Problem Solving, Control Methods and Search—*Heuristic Methods*;
I.4.5 [**Image Processing and Computer Vision**]: Reconstruction—*Transform Methods*

GECCO'07, July 7-11, 2007, London, England, United Kingdom

General Terms

Algorithms, Design

Keywords

Genetic algorithms, wavelets, image processing

1. INTRODUCTION

Image and signal processing are active areas of defense and security research. Satellites and Unmanned Aerial Vehicles (UAVs) collect copious amounts of image data during surveillance missions. Likewise, sonar and radar systems process huge amounts of sensor data in real time. The requirements to maximizing effectiveness while minimizing mission cost necessitates compression strategies that minimize storage and bandwidth requirements while maintaining maximum signal information.

With these requirements in mind, quantization of data is often necessary for military digital signal processing (DSP) applications. *Quantization* minimizes storage requirements by mapping all values in signal γ to a restricted discrete set of values $Q(\gamma)$. Though quantization greatly improves compression ratios, perfect reconstruction of γ from $Q(\gamma)$ is impossible due to the loss of low-order bits [18]. *Wavelets* [3] are a standard methodology for signal compression algorithms. The discrete wavelet transform (DWT) redistributes the energy in a signal by transforming a time signal into a time-frequency domain. A signal may be compressed by first applying the DWT, followed by quantization, and then by applying entropy coding. Signals are reconstructed in a reverse manner. Most information loss occurs during quantization[1].

In recent years, evolutionary algorithms have been employed in conjunction with wavelets for a variety of image and signal processing applications. In [8], a GA con-

[1]Further information on the wavelet transform and quantization as they relate to this research may be found in our GECCO main conference paper [14].

trols wavelet-based signal approximation. Grasemann and Mikkulainen use a GA to control the design of a lifting-based wavelet for signal compression [5]. In [10], a real-coded GA to replaces DWT filter coefficients for the reconstruction of quantized one-dimensional signals, including ramp functions, sine waves, and sets of randomly generated noise, demonstrating consistent MSE improvement over signals reconstructed using a Daubechies-4 (DB4) inverse discrete wavelet transform (DWT^{-1}) filter. As wavelets have become a popular tool for image processing [15], evolutionary techniques have been used with wavelets for a number of applications. Bruckman et al. [1] employ a binary GA to evolve structures for wavelet packet based image compression [19]. The GA replaces the best basis algorithm [2] for selecting the wavelet basis structure, resulting in reduced distortion during compression. Image texture classification may be accomplished by configuring a Kohonen self organizing map (SOM) with a GA in conjunction with a wavelet-based filter [16]. In [6], a GA applies the lifting technique to design complementary wavelet filters [17]. The evolved wavelets outperform the standard FBI wavelet [7] for fingerprint image compression.

In recent related research, a GA evolves digital filters by initializing the GA population with values near the original DWT filter and then searching for improved filters in the neighborhood of the original wavelet through a local mutation mechanism [9]. The GA successfully improves image reconstruction both when evolving a single filter for all MRA levels or when evolving unique filters for each level of MRA wavelet decomposition. In related work, a GA evolves only the reconstruction coefficients of a wavelet-based filter to improve image reconstruction in the presence of quantization error [11]. By focusing on the evolution of optimized reconstruction coefficients, the underlying compression rate of the forward transform is unaffected. However, the resulting filters described in [11, 9, 12] are no longer wavelets because they no longer conform to the mathematical properties of wavelets, such as biorthogonality of the filters. Evolved with one or more training images, the resulting filters provide improved reconstruction when applied to images not explicitly represented by the training image population.

While GAs provide filters providing improved reconstruction over DWT filters in applications subject to quantization error [11, 12], filters must be trained using images appropriate for the target application. An evolved transform filter trained using images of human faces may not provide sufficient reconstruction of an overhead image of a city captured from a high altitude. The evolution of image transforms for satellite and UAV applications requires a set of appropriate images for GA training and validation testing of resulting filters. This paper describes a set of fifty unclassified satellite images depicting the types of subjects that may be observed during a surveillance mission. Such targets may include cities, factories, airstrips, and military bases and vessels. Experiments identify the best GA training images within the set providing transform filters that demonstrate strong performance across the entire image set. The remaining images are used to validate the performance of evolved filters. Military image processing systems may benefit from evolved transforms developed and validated with this image set.

2. COLLECTED SATELLITE IMAGES

Quantization error may occur in image processing systems requiring transmission of data through a limited bandwidth. Micro-unmanned aerial vehicles (mUAVs) and deep-space exploration satellites represent two possible applications for image compression and transmission subject to quantization error. In order to demonstrate the practical applications of image transform filters evolved to handle quantization error, we have assembled fifty high-resolution satellite images from Google Earth Plus [4]. These public domain images are intended to simulate the type of targets observed by a mUAV during an intelligence-gathering mission. The purpose of gathering such images is to demonstrate that filters can be evolved to provide improved reconstruction over standard wavelets when subject to quantization, hence maximizing the amount of intelligence preserved from the original target.

This collection categorizes the images into the following categories: army (five images), aviation (twelve images), city (nine images), factory (five images), industry (five images), landmark (three images), and naval (eleven images). The images are captured from a variety of global locations. Upon identifying appropriate images in GoogleEarth, the images were first captured and printed to a pdf file using Adobe Acrobat with the high-quality print settings enabled. This allows higher-resolution image capturing than would be possible through a screen-shot capture using standard GoogleEarth software. The images were next extracted from the pdfs as full color bitmap images. Each image was then cropped to 512x512 pixels. After cropping, images were converted to greyscale representation. Using histogram adjustment tools in Adobe Photoshop, the pixel ranges of the greyscale cropped images are adjusted to cover the full range of 0-255 (black to white) shades. Hence, each pixel in each image is represented by an unsigned eight-bit integer.

Figure 1 presents six representative images in the collection. From left to right, the top row shows views of the U.S. Army Depot in Anniston, AL, Hopkins International Airport in Cleveland, OH, USA, and a downtown view of Moskow, Russia. The bottom row presents a factory near Detroit, MI, USA, the U.S. capitol building in Washington, DC, USA, and the U.S. Coronado Naval Base in California. Images were selected for inclusion in this set based upon clear focus, appropriate contrast, varieties of textures and object edges, and potential intelligence images. The performance of evolved transforms designed for aerial and satellite applications may be validated through strong performance across these images.

3. IMAGE RANKING EXPERIMENTS

Some satellite images may represent difficult training examples. A GA may overtrain a filter for a specific satellite image that does not perform well on other unseen images. Likewise, some satellite images may encourage the evolution of robust filters that provide improved image reconstruction over unseen images. An initial series of experiments identify the satellite images that when employed as GA training examples result in filters providing consistent reconstruction improvement over the entire set of satellite images. In order to assess each image in terms of its usefulness as a training image and as a test image, we conduct one GA run for each image using standard operators that provided consistent solid performance in previous research [12].

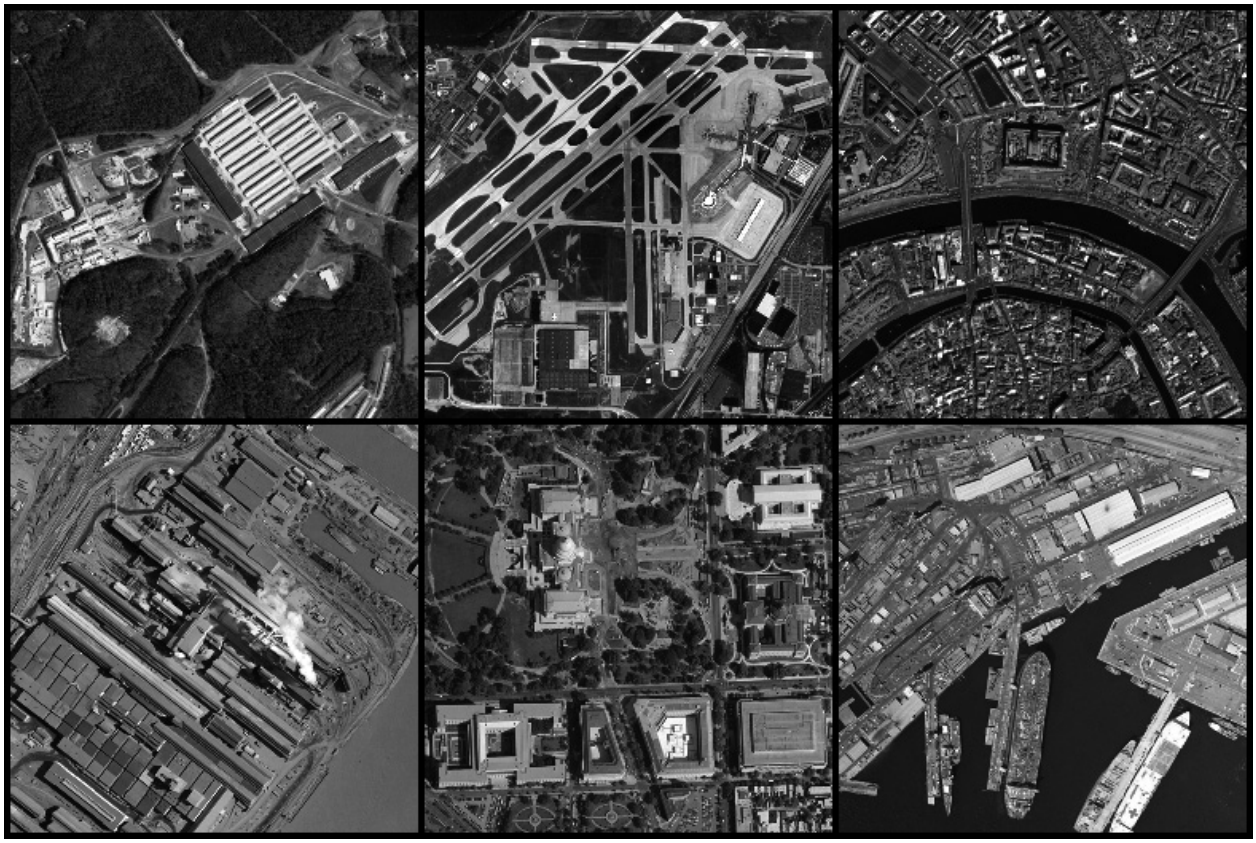

Figure 1: Six representative satellite images.

Experiments are conducted using a GA previously demonstrating successful filter evolution [12, 14]. The GA employs a population size of 50 evolved for 500 generations. The population is initialized in the local neighborhood of the Daubechies-4 (DB4) reconstruction wavelet transform to ensure that the final evolved filter will be at worst equal to the original wavelet filter. The GA replaces the eight real-valued coefficients defining the DB4 filter with eight evolved coefficients representing a new filter. Evolution occurs through the use of Gaussian mutation with standard deviations that shrink by generation, Wright's heuristic crossover [20], and random selection. In each generation, the two most fit parents survive to the next generation. Of the remaining individuals for the next generation, 70% are created through application of the crossover operator, while the remainder are mutated from a randomly selected parent. While a 30% mutation rate may seem high, we select this crossover to mutation ratio based upon initial empirical results from a set of parameter configuration experiments. Image reconstruction employs a quantization step size = 64 and employs a single level of filter decomposition. Fitness is assessed as the MSE between an image reconstructed using a candidate filter and the original image. Perhaps the simplest and most common image error measure, MSE provides a simple statistical measure to estimate the error of one image as an approximation of another. Let $x = \{x_i | i = 1, 2, ..., N\}$ and $y = \{y_i | i = 1, 2, ..., N\}$ represent the original and test images. The MSE between the test and original images is defined as:

$$MSE(x, y) = \frac{1}{n} \sum_{i=1}^{n} (x_i - y_i)^2 \quad (1)$$

An MSE = 0 in a reconstructed image indicates that image x is a perfect reconstruction of y; increasing values correspond to increasing error. An optimization algorithm improves reconstruction by minimizing MSE as an objective fitness measure.

Each of the resulting fifty filters is tested on all fifty images to find the average % MSE improvement over the DB4 wavelet of each filter. In order to track an image's performance as a test image, the average improvement of each image using all fifty evolved filters is also assessed. Table 1 presents the results of the fifty GA runs. For each image, the center columns present the rank of each image as a training image with the average and standard deviation of the % MSE improvement across all images. The right columns present the ranks of each image as test images with the average improvement of each image using all fifty evolved filters.

In general, the image test ranks are less important than the training ranks. Evolved filters only require one fitness evaluation for each test image to assess test performance, but training images are used in many fitness evaluations during GA execution. Thus, all satellite images can be used as test images during experimentation, but only one image will be used as a training image for each GA run. Based upon the initial experiments, the five best training images

#	image description	Rank as Training Image			Rank as Test Image		
		rank	% improve	stDev	rank	% improve	stDev
1	AF museum	48	5.4136	5.3643	2	20.5945	2.6381
2	Andrews AFB	35	13.262	2.5424	3	19.4647	4.4735
3	Anniston Depot	23	14.5365	1.9218	36	18.2435	4.1587
4	Anniston Bunkers	3	15.1135	1.7327	28	18.4761	4.3326
5	Baghdad	21	14.64	1.9437	4	19.3658	6.2281
6	Baghdad Landmarks	4	15.0648	1.8919	7	19.157	5.302
7	Boeing Factory	6	15.0557	1.8574	16	18.9026	4.373
8	Boneyard Kingman	1	15.1801	1.8258	31	18.4002	4.5763
9	Buildings New York	33	13.8357	1.7385	38	17.9002	5.4082
10	Chrystler Plant	25	14.4147	1.9644	8	19.1339	7.8508
11	Cleveland Hopkins	28	14.2994	1.7806	14	19.0006	7.2664
12	Coronado 1	42	10.7273	2.3244	48	15.1126	4.6989
13	Coronado 2	22	14.6084	1.8567	19	18.871	5.5468
14	Coronado 3	8	15.0045	1.8522	21	18.7499	5.4681
15	Davis Monthan	30	14.1424	1.9358	33	18.3491	4.3869
16	Davis Monthan B-52s	45	10.1868	3.5754	5	19.3151	4.0291
17	Downtown Munich	5	15.0577	1.6874	22	18.6956	5.4984
18	Downtown New York	14	14.8791	1.7259	13	19.0422	6.4994
19	Factory Detroit	15	14.8639	1.6726	35	18.2444	5.6603
20	Factory Toledo	9	14.9947	1.8385	10	19.0857	6.1791
21	Fort Dix	37	12.1275	2.0705	30	18.4305	3.0378
22	Fort Hood	10	14.9546	1.6536	24	18.6355	5.8032
23	Fort Hood Grounds	2	15.1217	1.7724	32	18.3683	4.1118
24	Groom Lake	50	-9.4513	11.0795	1	22.1512	4.046
25	Industry Detroit	16	14.8565	1.711	17	18.898	4.8943
26	Iron Cleveland	7	15.0442	1.6863	25	18.618	5.4687
27	Kastellet	36	12.3594	2.7449	41	16.5978	3.0789
28	Kennedy Space Center	29	14.1568	1.8264	12	19.0494	3.2167
29	Kennedy Launchpad	39	11.813	1.3876	45	16.0652	4.4106
30	Moskow	24	14.5349	1.8334	15	18.9238	6.9282
31	Munich Train	12	14.8856	1.7284	26	18.5579	3.9602
32	Naval Air Norfolk	32	14.005	1.8038	40	17.2317	3.5275
33	Naval Norfolk Ships	41	11.2327	2.6551	44	16.1823	2.9996
34	Naval Station Norfolk	46	9.0476	3.0051	47	15.9651	3.1672
35	Naval Station Carriers	38	11.8479	2.4575	43	16.3971	3.2486
36	Oil Refinery	17	14.8259	2.1066	18	18.893	6.5343
37	Pearl Harbor Subs	47	6.7446	2.1814	50	12.286	5.8306
38	Pearl Harbor Drydock	20	14.6551	2.1422	20	18.7886	6.5201
39	Pearl Harbor Complex	43	10.6317	2.7398	42	16.5756	6.8539
40	Pinal Airpark	26	14.3444	2.0629	37	17.9472	4.988
41	Seattle Harbor	40	11.6195	2.8656	46	16.0181	3.6441
42	Ships Pearl Harbor	49	-1.3824	5.4811	49	13.4913	3.793
43	Steel Baltimore	18	14.7206	1.7574	11	19.0521	5.2634
44	Steel Cleveland	27	14.3219	2.1419	27	18.4938	3.4355
45	St. Louis Downtown	31	14.0496	1.8938	29	18.4361	4.4393
46	US Capitol	13	14.8822	1.8507	23	18.657	4.2602
47	Washington DC	11	14.8929	1.7728	6	19.3083	6.173
48	WPAFB area A	44	10.5765	2.2597	39	17.6422	2.749
49	WPAFB area B	19	14.6701	1.7393	34	18.3005	2.6796
50	WSU	34	13.8026	1.8673	9	19.1274	3.332

Table 1: Initial ranks of satellite images as GA training and test images.

each have significant object edges. A wavelet filter will typically produce a large response at the edges in an image due to the convolution involved in the DWT algorithm. It is not overly surprising that the best training images contain more edges (high-spacial frequency information) than the worst images that are typically edge-sparse. The presence of edges in a training image allow the GA to develop filters with an appropriate response to both the high-spacial frequency portions of images (i.e. strong edges) as well as the lower frequency areas (weak or non-edges).

4. VALIDATION EXPERIMENTS

The training ranks obtained in the initial experiment are the result of a single GA run for each image. While the approximate rank of each image relative to the entire image set is probably close to its true rank, statistical validation through experiment replication is required to provide a more accurate ranking. Hence, the average improvement obtained with filters trained on the top five images is reassessed through a set of replicated experiments. Thirty GA experiments are conducted with each of the top five images. The GA and fitness function both employ the same parameters used in the initial ranking experiments.

Results of the replication experiments are shown in table 2. Average GA MSE and % Improve show the average improvement of the training image with the final filter across all thirty replications. More importantly, the % test imp column gives the average improvement of all fifty satellite images across all thirty replications conducted for each of the top five training images. After the replication experiments, image 6 (Baghdad Landmarks) provides the best performance, providing filters that improve the reconstruction MSE of all satellite images by an average of 15.145%. Two-sided student's t-tests at a significance level $\alpha = 0.5$ between replication experiments for each of the top five images indicate that the average test % improvement is significantly different between each replication set except for that of images 4 and 17. After conducting the replication validation experiments, the ranks of the top five images are revised. Image 6 becomes the top-ranked training image. Image 8 moves down one position to rank two, while image 4 remains the third-ranked training image. Image 17 moves up from the fifth to the fourth ranked training image, while image 23 is now ranked fifth. Figure 2 shows the top four validated training images: landmarks in Baghdad, Iraq (image 6, top left), bunkers at the U.S. Army Depot in Anniston, AL (image 4, top right), the aircraft boneyard in Kingston, AZ,USA (image 8, bottom left), and downtown Munich, Germany (image 17, bottom right). In general, image transforms evolved on one of the top ranking training images will exhibit strong performance across the entire satellite image set. Such transforms are well-suited for use in satellite and UAV reconnaissance applications requiring the transmission of copious amounts of image data across limited bandwidth channels.

5. CONCLUSIONS AND FUTURE WORK

The development of military-grade image transforms for reconnaissance missions requires a robust set of domain-appropriate images to train and validate evolved transforms. From a collection of fifty unclassified images, experiments successfully identify five training images that permit a GA to develop reconstruction transforms providing an average MSE reduction of approximately 15% over the DB4 DWT^{-1} under high quantization over the entire image set. Images from this collection are already being employed in the development of an evolutionary methodology for the creation of image transform filters intended for defense and security applications [14, 13]. By including images with a variety of textures, shades, and domain-appropriate structures and subjects, this collection provides a suitable testbed for defense-oriented image transforms.

Figure 2: The four best satellite training images.

In related research, we exploit edge detection for the targeted improvement of edge transition areas in images [14]. This research employs selected images from this collection to develop image transforms focused upon accurate reconstruction of object edges within satellite images. As this research proceeds, we will conduct experiments to rerank the images for usefulness in producing high frequency filters for improving image edges We will initially conduct one GA experiment with each of the 50 satellite images, followed by a set of thirty GA replications for each of the top five ranked images. The top-ranked images will be used to develop increasingly sophisticated filters suitable for defense applications in image processing and intelligence analysis.

6. REFERENCES

[1] A. Bruckmann, T. Schell, and A. Uhl. Evolving subband structures for wavelet packet based image compression using genetic algorithms with non-additive cost functions. In *Proceedings of the International Conference on Wavelets and Multiscale Methods*, 1998.

[2] R. Coifman and V. Wickerhauser. Entropy-based algorithms for best basis selection. *IEEE Transactions on Information Theory*, 38:713–718, 1992.

[3] I. Daubechies. *Ten Lectures on Wavelets*. SAIM, 1992.

[4] Google. Google earth plus. http://earth.google.com/, 2006.

Best 5 Training Images Validation Results

Image	Daub4 MSE	Avg GA MSE	StDev	% Improve	stDev	% test imp	stDev
8	178.138	149.53	0.233	16.06	0.131	15.09	0.095
23	151.841	129.822	0.327	14.501	0.216	14.826	0.273
4	183.187	153.203	0.315	16.368	0.172	15.009	0.151
6	194.078	159.967	0.176	**17.576**	0.091	**15.145**	0.081
17	162.384	137.43	0.225	15.368	0.139	14.968	0.124

Table 2: Validation results for five best satellite images. % improve shows the average % MSE improvement of the training image over 30 GA runs. % test improve shows the average improvement over all 50 test images across 30 GA runs.

[5] U. Grasemann and R. Miikkulainen. Evolving wavelets using a coevolutionary genetic algorithm and lifting. In *Proceedings of the Genetic and Evolutionary Computation Conference - GECCO-04*, volume 3103 of *Lecture Notes in Computer Science*, pages 969–980. Springer-Verlag, 2004.

[6] U. Grasemann and R. Miikkulainen. Effective image compression using evolved wavelets. In *Proceedings of the Genetic and Evolutionary Computation Conference (GECCO'05)*, pages 1961–1968, 2005.

[7] T. Hopper, C. M. Brislawn, and J. N. Bradley. Wsq gray-scale fingerprint image compression specification. Technical Report IAFIS-IC-0110, Federal Bureau of Investigation, February 1993.

[8] M. Lankhorst and M. van der Lann. Wavelet-based signal approximations with genetic algorithms. In *Proceedings of the 4th Annual Conference on Evolutionary Programming*, pages 237–255, 1995.

[9] F. Moore. A genetic algorithm for evolving improved mra transforms. *WSEAS Transactions on Signal Processing*, 1(1):97–104, 2005.

[10] F. Moore. A genetic algorithm for optimized reconstruction of quantized signals. In *IEEE Congress on Evolutionary Computation (CEC) Proceedings vol. 1*, pages 105–111, 2005.

[11] F. Moore, P. Marshall, and E. Balster. Evolved transforms for image reconstruction. In *IEEE Congress on Evolutionary Computation (CEC) Proceedings vol. 3*, pages 2310–2316, 2005.

[12] M. R. Peterson, G. B. Lamont, and F. Moore. Improved evolutioanry search for image reconstruction transforms. In *Proceedings of the IEEE World Congress on Computational Intelligence*, pages 9785–9792, 2006.

[13] M. R. Peterson, G. B. Lamont, F. Moore, and P. Marshall. Evaluating variation operators for evolved image reconstruction transforms. In *SPIE Defense and Security Symposium, Orlando, USA*, 2007. *To Appear.*

[14] M. R. Peterson, G. B. Lamont, F. Moore, and P. Marshall. Targeted filter evolution for improved image reconstruction resolution. In *Genetic and Evolutionary Computation Conference, London, UK*, 2007. *To Appear.*

[15] A. A. Petrosian and F. G. Meyer. *Wavelets in Signal and Image Analysis*. Kluwer Academic Publishers, 2001.

[16] B. S. Rani and S. Renganathan. Wavelet based texture classification with evolutionary clustering networks. In *TENCON 2003: IEEE Conference on Convergent Technologies for Asia-Pacific Region*, volume 1, pages 239–243, 2003.

[17] W. Sweldens. The lifting scheme: a custom-design construction of biorthogonal wavelets. *Journal of Aplied and Computational Harmonic Analysis*, 3(2):186–200, 1996.

[18] B. E. Usevitch. A tutorial on modern lossy wavelet image compression: foundations of jpeg 2000. *IEEE Signal Processing Magazine*, pages 22–35, September 2001.

[19] M. Wickerhauser. *Adapted Wavelet Analysis from Theory to Software*. A. K. Peters, 1994.

[20] A. H. Wright. Genetic algorithms for real parameter optimization. In G. Rawlins, editor, *Foundations of Genetic Agorithms*, pages 205–220, San Mateo, 1991. Morgan-Kaufman.